The Role of Apelin/APJ in a Mouse Model of Oxygen-induced Retinopathy

Jing Feng,[1,3] Li Chen,[1] Yanrong Jiang,[2] and Yong Tao[1]

[1]Department of Ophthalmology, Beijing Chaoyang Hospital, Capital Medical University, Beijing, China
[2]Department of Ophthalmology, People's Hospital, Peking University, & Beijing Key Laboratory of Diagnosis and Therapy of Retinal and Choroid Diseases, Beijing, China
[3]Department of Ophthalmology, PLA Rocket Force General Hospital, Beijing, China

Correspondence: Yanrong Jiang, Department of Ophthalmology, People's Hospital, Peking University, 11 Xizhimen South Street, Xicheng District, 100044, Beijing, China; drjyr@vip.sina.com.
Yong Tao, Department of Ophthalmology, Beijing Chaoyang Hospital, Capital Medical University; No. 8, South Road of Worker's Stadium, Chaoyang District, Beijing 100020, China; taoyong@bjcyh.com.

JF and LC contributed equally to this study.

Received: June 16, 2019
Accepted: May 20, 2020
Published: July 30, 2020

Citation: Feng J, Chen L, Jiang Y, Tao Y. The role of apelin/APJ in a mouse model of oxygen-induced retinopathy. *Invest Ophthalmol Vis Sci.* 2020;61(8):47. https://doi.org/10.1167/iovs.61.8.47

Purpose. The aim of this study was to investigate apelin and its potential neovascularization role in retinopathy of prematurity (ROP) along with the inhibitory effects of its antagonist.

Methods. We used an oxygen-induced retinopathy (OIR) mouse model to explore the progress of ROP. Apelin and angiotensin receptor-like 1 APJ expressions were examined in the retina using immunohistochemistry, quantitative polymerase chain reaction, and Western blot analysis. Additionally, the retina was examined by whole-mount staining to evaluate the retinal vessel area, vessel density, capillary width, and the number and length of tip cells. The expression of the phosphorylated mTOR (p-mTOR), p-PI3K/Akt, and p-Erk signaling pathway was also evaluated using Western blot analysis.

Results. Apelin promoted the development of superficial and deep retinal blood vessels, especially for tip cells during the physical development of retinal vessels. Additionally, apelin stimulated the density of the peripheral retinal zone vessels in OIR mice. The apelin and APJ expression levels significantly increased for the OIR model during their hypoxic phase. Next, we found that apelin mRNA levels in the OIR mice peaked at six hours after return to ambient conditions at P12, whereas the APJ mRNA levels peaked later at P17. Furthermore, the expression of p-mTOR, p-Akt, and p-Erk were all up-regulated in OIR mice whereas F13A suppressed them instead.

Conclusions. Our results suggest that apelin/APJ signaling pathway is a key factor for hypoxia-induced pathologic angiogenesis, which is a very promising new target for the treatment of ROP.

Keywords: apelin, APJ, retinopathy of prematurity

Vascular endothelial growth factor (VEGF) has been considered the key mediator of ROP.[1,2] For instance, anti-VEGF therapy has proven to be effective in inhibiting neovascularization.[3,4] However, increasing evidence has revealed that anti-VEGF alone cannot prevent the occurrence of new vessels (NVs) completely, and has been associated with reactivation of ROP, indicating the involvement of other factors apart from VEGF regarding neovascularization.[5–7]

Apelin is a recently isolated bioactive growth factor from bovine gastric extract regarding as an endogenous ligand for angiotensin receptor-like 1 APJ and able to mediate angiogenesis and vascular formation.[8] It has been reported that apelin is required for both developmental and pathogenic nonneovascular remodeling.[9] In our previous study, we examined the expression of apelin and APJ in clinical samples from infants.[10] We also reported that apelin and APJ express in the fibrovascular membranes of infants with ROP; meanwhile, anti-VEGF treatment cannot inhibit apelin expression and cannot completely suppress retinal neovascularization, which infers that apelin may play an important role in neovascularization and cannot be replaced by VEGF.[11] Moreover, apelin siRNA suppressed the proliferation of endothelial cells, which was independent of the VEGF/VEGF receptor 2 signaling pathway.[12] However, the high expression of apelin was able to initiate angiogenesis, indicating that apelin plays an important role in the process of neovascularization.[13] Given that apelin has been considered a potent factor promoting angiogenesis, we conducted this study to explore the role of apelin in physical and pathological retinal vessel development and to detect the treatment effect with its specific antagonist F13A on the oxygen-induced retinopathy (OIR) mouse model in vivo.

Materials and Methods

Animals and Experimental Design

C57BL/6J mice (The animal Laboratory, Peking University People's Hospital, Beijing, China) were used as an in vivo model for our investigation All animals were kept in 12 hours dark and light cycles and were fed with standard chow and water. All animal protocols were approved by the Institutional Review Board of Peking University People's Hospital

and conformed to the Use of Animals in Ophthalmic and Vision Research statement of the Association for Research in Vision and Ophthalmology.

Two types of mice were used in this study: normal and OIR mice. The normal mice were divided into two groups: nontreated normal mice (n = 16) and apelin-treated normal mice (n = 16), which were treated by using an intraperitoneal injection with 20 nmol/kg of apelin. The mice were sacrificed at postnatal day 7 (P7) and P10, respectively. For the OIR mice, they were divided into two separate groups: nontreated OIR mice (n = 15) and treated OIR mice (n = 15), which were treated by using intravitreally injected with 2 µL of 1 mg/mL F13A. Meanwhile, normal mice (n = 15) were used as the control group. The mice were sacrificed at P17.

OIR Mouse Model

New retinal vessels were induced in newborn mice as described previously.[14] In brief, newborn mice at P7 were exposed to 75% ± 2% oxygen together with their nursing mother for five days (from P7 to P12). These incubation conditions induced vaso-obliteration and subsequent cessation of vascular development in the capillary beds of the central retina.[14] At P12, the mice were returned to ambient conditions, in which they stayed for five days (until P17: the day that the disease peaks). A condition of relative hypoxia was induced between P12 and P17, and extensive new retinal vessels developed in the mice. The mice were examined and sacrificed on the time points that depended on the experiment's design.

Drug Administration

For the normal apelin-treated group (n = 16), one group of mice (n = 8) was treated with 20 nmol/kg of apelin via intraperitoneal injection at P4, P5, and P6 and then sacrificed at P7. The other group (n = 8) was treated similarly but at P7, P8, and P9 and sacrificed at P10 instead.

For the OIR treated group (n = 15), the mice were injected—immediately after their five-day treatment of 75% oxygen at P12—intravitreally in the right eye with 2 µL of F13A (1 mg/mL). All the groups were examined at different time points (depending on the experimental design) for qualitative assessment of the retinal vasculature using immunofluorescence staining, quantitative real-time polymerase chain reaction (qRT-PCR), and Western blot analysis. Each assessment method was performed in triplicate for each experimental condition. The samples from age-matched control mice were used for comparison.

Retina Whole Mount Staining and Measurement of Neovascularization

Retinal whole mount staining was performed as previously described.[15,16] The eyes of normal mice were enucleated at P7 and P10 and were fixed in 4% paraformaldehyde for 30 minutes at room temperature. We removed the corneas and lenses first, then the eyecups were fixed in 4% paraformaldehyde for 10 more minutes. The retinas were carefully dissected and washed three times in phosphate-buffered saline solution (PBS) for 15 minutes. Retinal flat mounts were stained at 4°C overnight in 100 µL PBS containing 1% bovine serum albumin (BSA) and 1% Triton X-100 with at least one of the following primary antibodies: Lectin-FITC (L9381, 1:50, Sigma-Aldrich Corp., St. Louis, MO, USA) or Collagen IV (BP8019,1:100, Acris, Herford, Germany). Afterward, the following secondary antibodies, goat anti-rabbit 594, (1:200, Invitrogen, Carlsbad, CA, USA) were added for two hours in the same buffer. Then, the flat mounts were mounted on microscopic slides and cut into four quadrants. Finally, microscopic images (original magnification × 16) were taken of the stained samples using a fluorescent microscope (Leica DMRBE, Bensheim, Germany) which was equipped with the IM50 software. The vessel area of P7 and P10 were measured with image processing software Cell F (Olympus, Hamburg, Germany).

To analyze the development of superficial retinal vessels at P7 and "both superficial and deep retinal vessels" at P10, images were taken with the Olympus BX51 microscope. Six to eight fields (original magnification × 200) between the arterioles and venules were randomly chosen. The growth of vessel network was evaluated by measuring capillary density (vessel/retinal area ratio) and width, which were quantified using Cell F software (Olympus).

Numbers of tip cell were counted manually by counting the numbers of sprouts at P7 (original magnification × 200) or branchpoints at P10 (original magnification × 100) in six to eight fields for each retina under the fluorescence microscope. The length of tip cell was measured from the edge of the bottom area to the end of the sprout at P7 (original magnification × 400) and at P10 (original magnification × 200), which were quantified using Cell F software (Olympus).

We defined the zones imitating the classification of ROP. "Central zone" is defined as a circle, centered on the disc, whose radius is 500 µm from the disc; "Middle zone" is from the edge of "Central zone" to the circle, whose radius is 1000 µm from the disc; "Peripheral zone" is the remaining area out of circle of 1000 µm from the disc (Fig. 1).

Immunohistochemistry of the Retina

Apelin's expression and location were determined in retinas from mice grown in the ambient and the hyperoxia conditions (with 10 mice in each group). The enucleated eyes were embedded in optimum cutting temperature compound (Tissue-Tek, Sakura Finetek Inc, Tokyo, Japan) and directly frozen in a cryostat (Leica CM1900, Berlin, Germany) at −20°C. Serial frozen sections of 8 µm were cut along the vertical meridian and then air-dried. The frozen sections were fixed in acetone for 10 min and then washed in PBS at room temperature. Next, a solution of 1% Triton X-100 and 1% BSA in PBS was added to permeabilize and block (against unspecific antibody binding) the retinal tissues for 1 h, respectively. Afterward, the primary antibody rabbit anti-apelin polyclonal IgG (No. ab59469, Abcam, MA, USA) at a dilution of 1:100 was added, and the Lectin-FITC antibody was added at 1:50 (L9381, Sigma, USA) at 4°C overnight. Afterward, the following secondary antibodies, goat anti-rabbit 594, (1:200; Invitrogen) were added for two hours in the same buffer. Finally, microscopic images were taken of the stained samples using a fluorescent microscope (Nikon 50i; Nikon, Tokyo, Japan).

Quantitative Real-Time PCR

The apelin/APJ mRNA levels were determined from mice grown in ambient and hyperoxia conditions (10 mice in

Investigative Ophthalmology & Visual Science

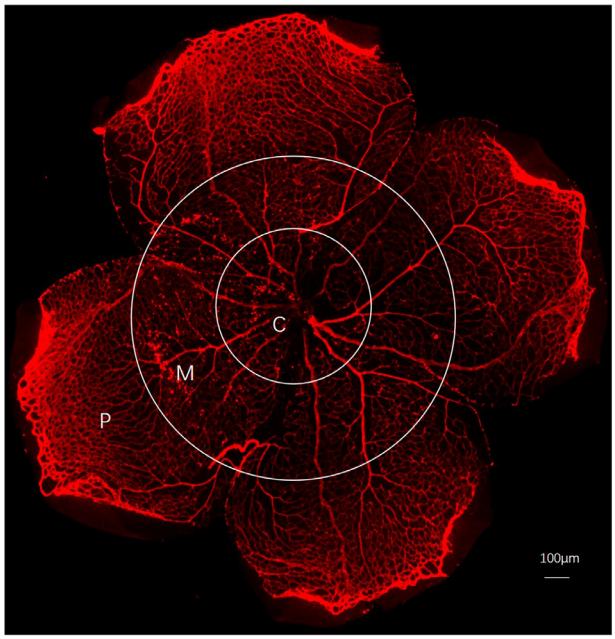

Figure 1. The schematic representation of the central, middle and peripheral retinal zones in mice. "Central zone" is defined as a circle, centered on the disc, whose radius is 500 μm from the disc; "Middle zone" is from the edge of "Central zone" to the circle, whose radius is 1000 μm from the disc; "Peripheral zone" is the remaining area out of circle of 1000 μm from the disc. *C*, central zone; *M*, middle zone; *P*, peripheral zone.

each group). First, the mice were euthanized, and their retinas were removed. Then the total RNA was isolated using the Trizol reagent (Invitrogen). The RNA concentration and integrity were determined with the Nanodrop 2000C UV spectrophotometer (Thermo Fisher Scientific, Waltham, MA, USA). Next, a Fermentas reverse transcription system (Fermentas, St. Leon-Roth, Germany) was used to convert 1 μg RNA into cDNA by using a real-time PCR system (Piko-Real 96 PCR system, Thermo Fisher Scientific). To determine the expression of each target gene, 1 μL of cDNA (1:10 diluted) was first mixed with 1 μL (10 pmol) of specific primers, 3 μL of diethyl pyrocarbonate–water, and 5 μL of SYBR Select Master Mix (Invitrogen), representing a final volume of 10 μL. The following primers were used to target the genes of interest: β-actin Forward: 5″-TGG CTC TAT CCT GGC CTC ACT-3″, β-actin reverse: 5″-GCT CAG TAA CAG TCC GCC TAG AA-3″; mice apelin Forward: 5″- GAT GGA GAA AGG CGA AGA AAG-3″, mice apelin reverse: 5″-GGT GAG AGA TGA GAC CAC TTG T-3″, mice APJ Forward: 5″-CCA CCT GGT GAA GAC TCT CTA CA-3″, and mice APJ reverse: 5″-TGA CAT AAC TGA TGC AGG TGC-3″. Each sample was measured in triplicate. The standard PCR conditions included two minutes at 50°C and 10 minutes at 95°C, followed by 35 cycles of denaturing, annealing, and elongating at 95°C for 15 seconds, 60°C for 30 seconds, and 72°C for 30 seconds, respectively. The threshold cycle (CT) values were used to calculate the fold change of gene expression for the different samples using the $2(-\Delta\Delta CT)$ formula. The fold change of the apelin and APJ genes relative to the β-actin endogenous control gene were determined using the following equation: fold change = $2^{-\Delta}$ (ΔCT), where change in threshold cycle (ΔCT) = CT (gene of interest) − CT (β-actin) and Δ (ΔCT) = ΔCT (experiment group) − ΔCT (control group). All experiments were performed in duplicate.

Western Blot Analysis

Western blot analysis was performed on retinas from the OIR mice, age-matched nontreated normal mice, and the F13A treated group. Each group contained retina tissue of 15 eyes from 15 mice. Western blot analysis for mammalian target rapamycin protein (p-mTOR), phosphoinositide 3-kinase (p-PI3K), protein kinase B (p-Akt), and extracellular signal-regulated kinases (p-Erk) was performed with cytosolic proteins, which were extracted using a buffer containing 0.1 mmol/L sodium orthovanadate, 20 mmol/L L-a -glycerophosphate, and 20 mmol/L p-nitrophenylphosphate. Aliquots of each sample containing equal amounts of protein were subjected to SDS-PAGE using 10% acrylamide gels. β-Actin was used as the loading control. The following primary antibodies were used: p-mTOR (1:1000, no. 2976, CST), p-PI3K (1:1000, no. 4228, CST), p-Akt (1:1000, no. 4060, CST), p-Erk (1:1000, no. 4370, CST), and β-actin (1:1000, no. 3700, CST). Then, as secondary antibodies, the mouse antirabbit horseradish peroxidase (1:6000 dilution) and rabbit antimouse horseradish peroxidase (1:6000 dilution) antibodies were used. The blots were treated with enhanced chemiluminescence reagent to visualize the bands. Afterward, the blots were stripped between each assay. All experiments were run in duplicate. Data from the different experiments were plotted and averaged in the same graph.

Statistical Analysis

Data in this study were expressed as the mean ± SD. Comparisons were made using Student's *t*-test for two groups or one-way analysis of variance followed by Bonferroni's post-hoc test; P values < 0.05 were considered statistically significant. The statistical analyses were performed using a statistical software package (SPSS for Mac, version 20.0; IBM, Armonk, NY, USA). Experiments were performed at least three times.

Results

Apelin Stimulated the Development of Superficial Retinal Vessels at P7

Our study focused on the early angiogenesis development in the retina of postnatal mouse. In the present study, the retinal vessels were stained for collagen IV, and the tip cells were stained for lectin. Figures 2A through 2C show that the area of the retinal vessels of apelin-treated mice was larger than the one from the PBS-treated group (2.274 ± 0.282 mm^2 vs. 1.579 ± 0.263 mm^2, $P < 0.01$). When comparing the capillary width of the peripheral retinal zone of the PBS-treated group with the apelin-treated one, the results were 5.51 ± 0.31 μm versus 3.91 ± 0.42 μm ($P < 0.001$), respectively (Figs. 2D–2F). Analyzing the density of retinal vessels revealed that the apelin-treated group had a higher density of vessels in the peripheral retinal zone than the PBS-treated one (51.31% ± 5.1% vs. 40.59% ± 4.5%; $P < 0.001$). No statistical significance was seen for the central and middle zones of the two groups ($P > 0.05$) (Figs. 2G, 2H).

We also determined the number of tip cells and their length in the whole-mounted retina. In apelin-treated group,

Investigative Ophthalmology & Visual Science

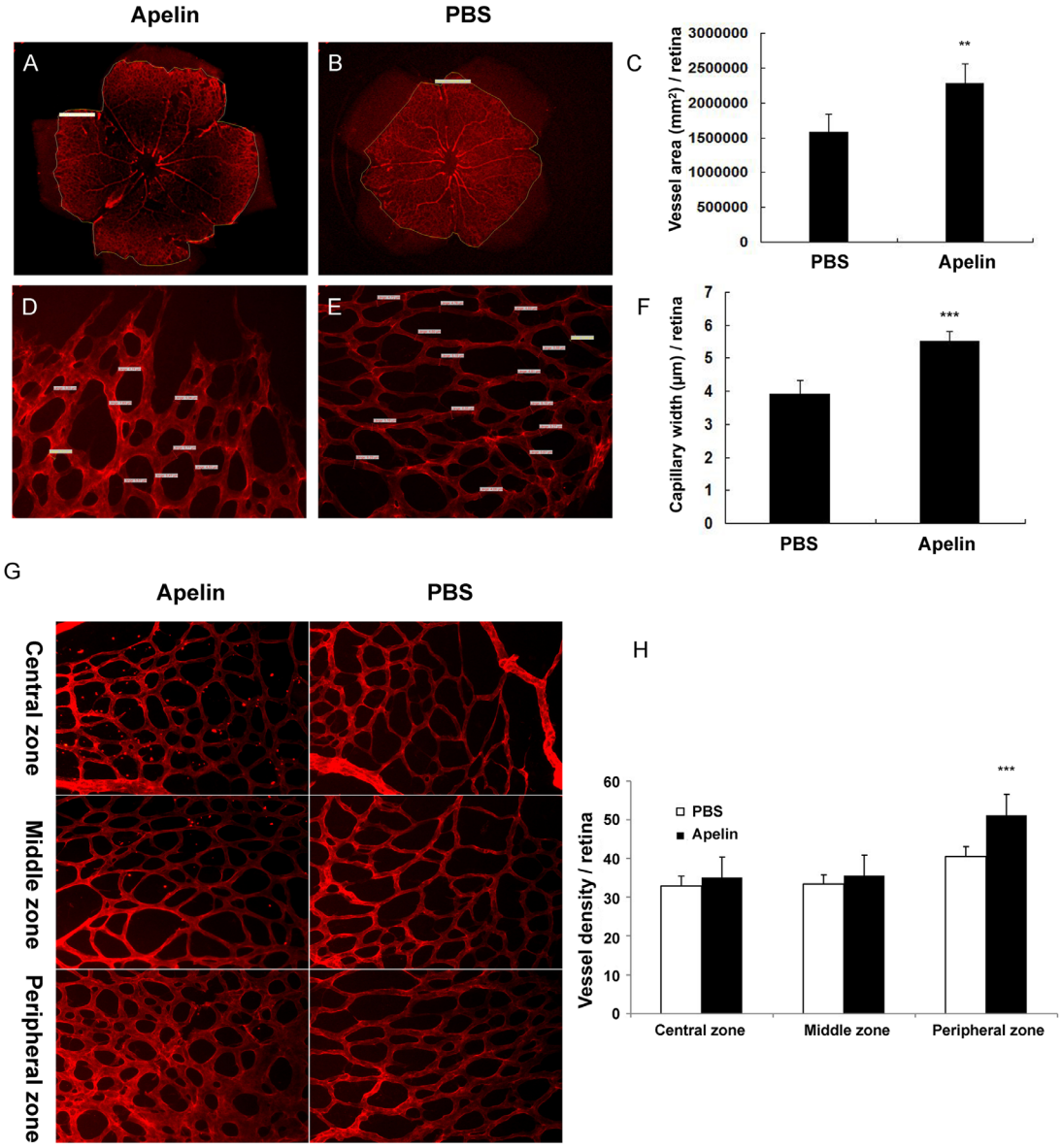

Figure 2. (**A, B**) Representative retinal whole mounts of various P7 mice injected intraperitoneally (P4, P5, and P6) with apelin (**A**) or PBS as control (**B**) showing the area of retinal vessels. Original magnification × 2.5. (**C**) Quantitative analysis of the area for retinal whole mounts (apelin-treated group vs. PSB-treated group, $^{**}P < 0.01$). (**D–F**) Retinal whole mounts that show the retinal capillary width in the apelin-treated (**D**) and PBS-treated group (**E**) of P7 mice. (**F**) Quantitative analysis of the retinal capillary width (apelin-treated vs. PSB-treated group, $^{***}P < 0.001$). (**G, H**) Representative retinal whole mounts that show the retinal vessel density of apelin-treated and PBS-treated mice at P7. Here, the vessel density in the central and middle zone in the apelin-treated group was similar to the PBS-treated group, whereas the vessel density in the peripheral zone was higher in the apelin-treated group ($^{***}P < 0.001$).

the number of tip cells was 37 ± 7.2 and only 24.4 ± 8.5 for the PBS-treated one ($P < 0.05$) (Fig. 3E). In the retina, exogenous apelin enhanced the tip cells' filopodia length (PBS-treated group 16.82 ± 1.94 μm vs. apelin-treated group 26.13 ± 2.55 μm, $P < 0.001$) (Fig. 3F).

Apelin Stimulated the Development of Deep Retinal Vessel at P10

Figures 4A through 4C show that the superficial area of retinal vessels at P10 was similar between the apelin-treated and the PBS-treated group (2.316 ± 0.202 mm^2 vs. 2.159 ± 0.287 mm^2; $P = 0.4$). However, no statistical significance was found for the superficial vessel density in the different zones between the two groups (Figs. 4D, 4E). The area of deep retinal vessels was measured. The results in Figures 4F and 4G show that the area was larger in the apelin-treated group than the PBS-treated group. However, there was no statistical significance between the two groups ($P > 0.05$). The tip cells were also detected and counted in the deep plexus. Here, the number of tip cells was 44.3 ± 5.2 in the apelin-treated and 37 ± 4.6 in the PBS-treated group ($P < 0.05$) (Fig. 5E). The tip cells had a longer length in the apelin-treated group ($P < 0.01$) (Fig. 5F).

Investigative Ophthalmology & Visual Science

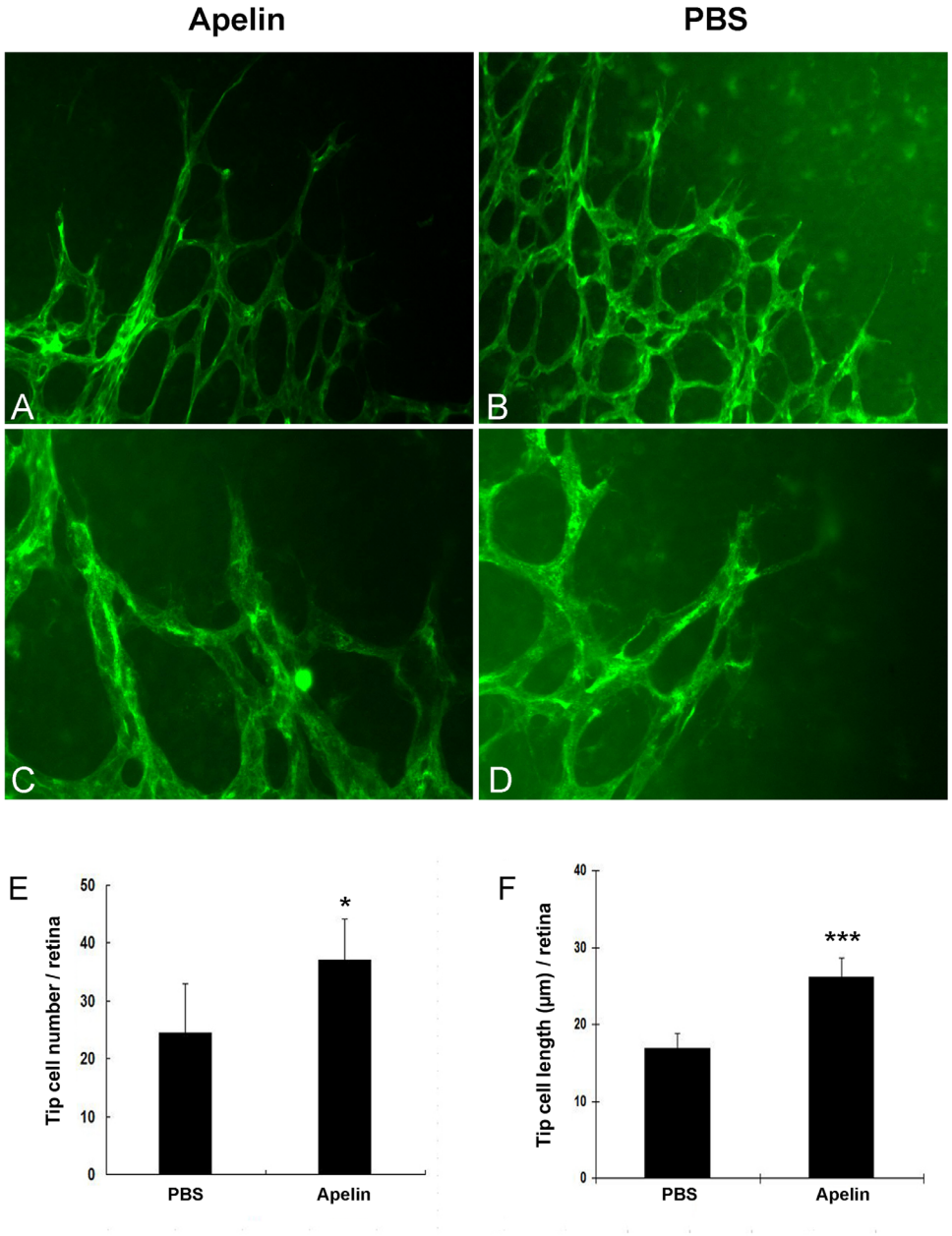

Figure 3. (**A–D**) Retinal whole mounts that show the retinal tip cells of the apelin-treated (**A, C**) and the PBS-treated group (**B, D**) at P7. (**E, F**) The quantitative number (**E**) and length (**F**) of the tip cells in two groups: the apelin-treated vs. the PSB-treated group (*$P < 0.05$, ***$P < 0.001$).

Measurement of Retinal Neovascularization in OIR Mice

After the role of apelin in the physical development of retinal vessels was investigated, we further studied the role of apelin in pathological angiogenesis. Staining of the whole-mount retina was used to evaluate the neovascularization after injecting apelin in OIR mice. The density of their retinal vessels was evaluated at P12. Figure 6 shows that the apelin-treated group had a higher density of vessels in the peripheral retinal zone compared with the PBS-treated group (35.4% ± 5.2% vs. 25.0% ± 4.0%, $P < 0.01$). However, there was no statistical significance in the middle zone between the two groups (25.4% ± 7.4% vs. 21.6% ± 6.7%, $P = 0.4$).

The Expression of Apelin and APJ was Up-Regulated in OIR Mice

As shown in Figure 7, the expression of apelin in the retina was up-regulated at P17 in OIR mice, illustrated by a more intense red staining—located in the ganglion cell layer, inner nuclear layer, and the vessel wall. In the normal mice, apelin was expressed less in the ganglion cell layer and inner nuclear layer.

Investigative Ophthalmology & Visual Science

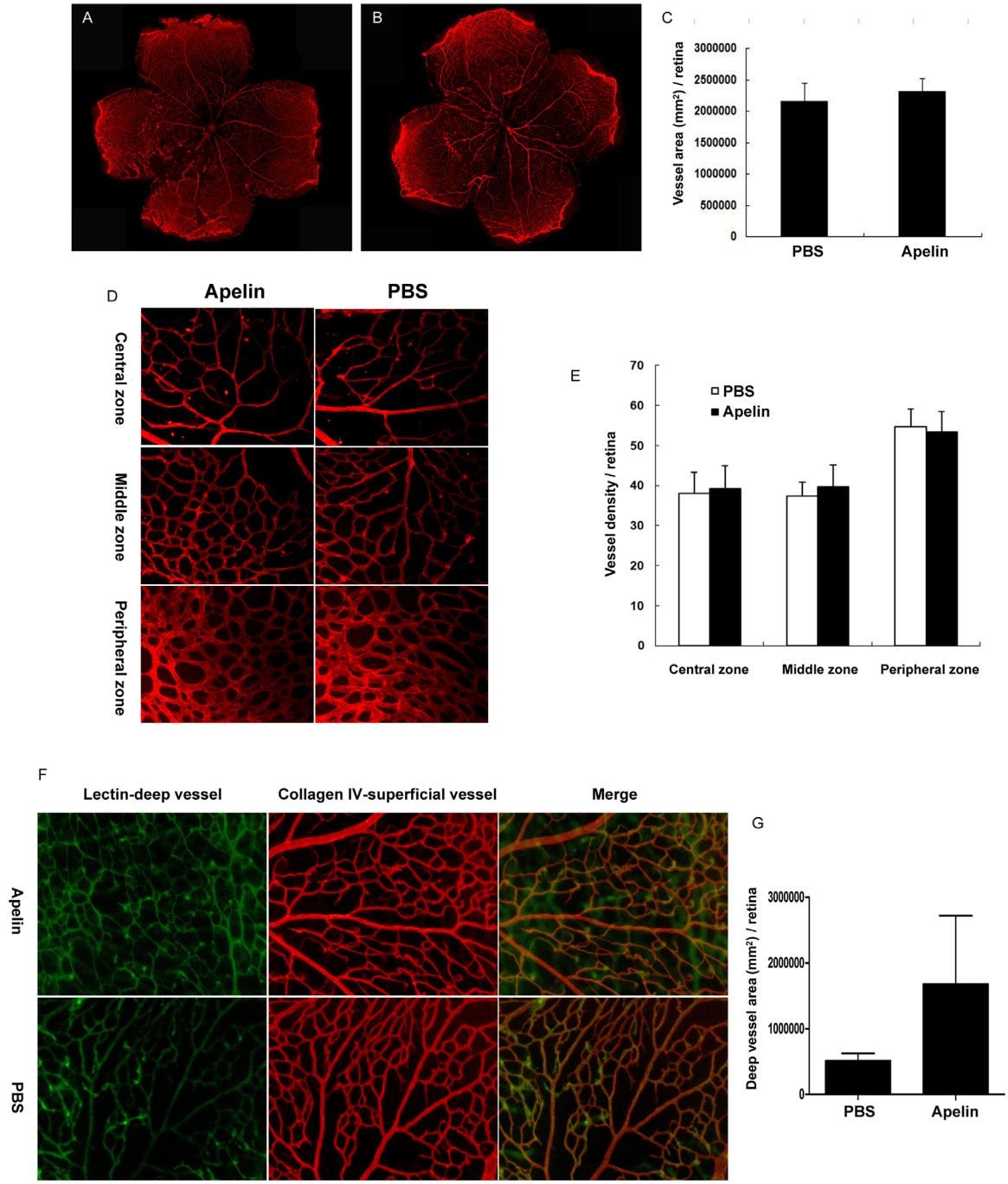

Figure 4. (**A–C**) Representative retinal whole mounts that show the superficial area of the retinal vessels of intraperitoneally injected mice (P7, P8, and P9) with apelin (**A**) or PBS (**B**) at P10. Original magnification × 2.5. (**C**) Quantitative analysis of the area for retinal whole mounts at P10 (apelin-treated vs. PSB-treated group, $p > 0.05$). (**D**) Representative retinal whole mounts that show the retinal superficial vessel density for apelin-treated and PBS-treated mice at P10. The vessel density in the central, middle, and peripheral zone in the apelin-treated group was similar to the PBS-treated one. (**E**) Quantitative analysis of the superficial vessel density for retinal whole mounts at P10. (**F, G**) Representative retinal whole mounts that show the area of deep retinal vessels in the apelin-treated group and the PBS-treated group at P10. (**F**) The deep vessels were stained with Lectin-FITC, and the superficial vessels were stained with Collagen IV. (**G**) Quantitative analysis of the area of deep retinal vessels.

The mRNA and Protein Expression of Apelin and APJ Are Increased in OIR Mice

Results from the qRT-PCR analysis show that from P5 and P12, apelin and APJ mRNA levels were gradually increased in the normal mice and peaked at P14 (Figs. 8A, 8C). Moreover, during the hypoxia stage, the apelin and APJ mRNA levels were significantly increased compared with the normal mice. Here, the mRNA level of apelin increased earlier than that of APJ in OIR mice. The apelin mRNA level peaked at six hours after return to ambient conditions at P12, whereas the APJ mRNA level peaked later at P17 in OIR mice (Figs. 8B, 8D).

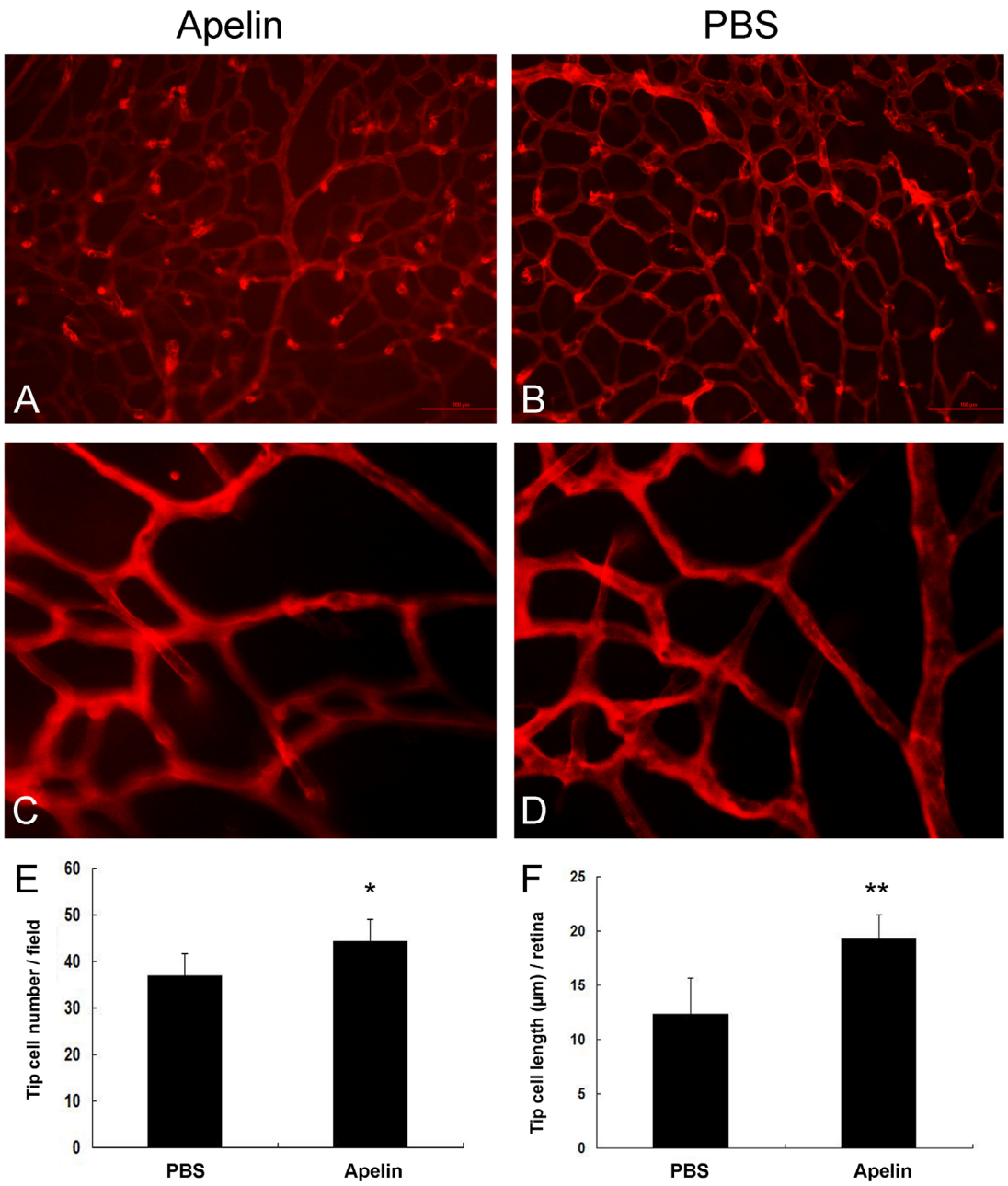

Figure 5. (**A–D**) Retinal whole mounts that show the retinal tip cells of the apelin-treated (**A, C**) and the PBS-treated group (**B, D**) in P10 mice. (**E, F**) The quantitative number (**E**) and length (**F**) of the tip cells from two groups (apelin-treated vs. PSB-treated group, $^{*}P < 0.05$, $^{**}P < 0.01$).

The Expression of mTOR, PI-3K, Akt, and Erk Are Altered After Injection of F13A

The expression changes of mTOR, PI-3K, Akt and Erk were observed after application of the APJ antagonist F13A. The protein expression was compared in the normoxia, OIR, and F13A-treated groups by Western blot. The results showed that compared with the normoxia group, the expression of p-mTOR, p-Akt, and p-Erk were up-regulated in the OIR group (Fig. 9). In the treated OIR group, the expression of the three proteins decreased significantly compared to the untreated OIR group (Fig. 9). However, the expression of PI-3K did not differ between groups.

Discussion

Studies showed that apelin/APJ is widely distributed in various tissues and that the apelin/APJ signal regulates pathological and physiological angiogenesis.[17–20] Our study demonstrated that exogenous apelin stimulated the tip cells' growth and promoted the development of retinal vessels in a physical manner. In a pathological condition, apelin enhanced retinal vessel growth and promoted angiogenesis, resulting in the acceleration of pathological development. Furthermore, the mRNA expression of apelin peaked first in OIR mice, followed by the APJ ones. The expression of p-mTOR, p-Akt, and p-Erk was attenuated

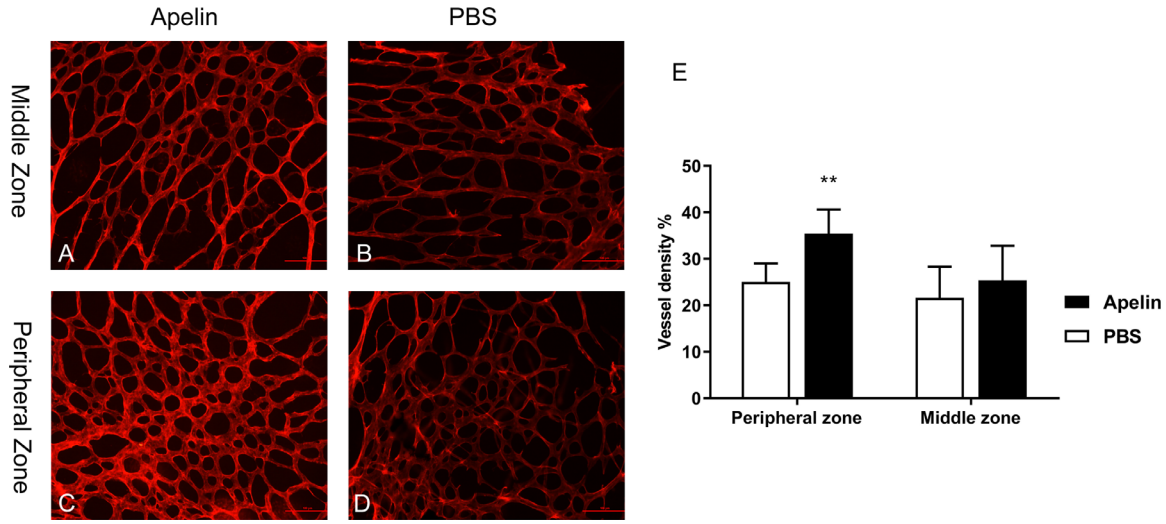

Figure 6. The retinal vessel density in OIR mice at P12. The apelin-treated group shows a higher density of vessels in the peripheral retinal zone than the PBS-treated group (35.4 ± 5.2% vs. 25.0% ± 4.0%, $^{**}P < 0.01$). However, there was no statistical significance for the middle zone between the two groups (25.4% ± 7.4% vs. 21.6% ± 6.7%, $P = 0.4$).

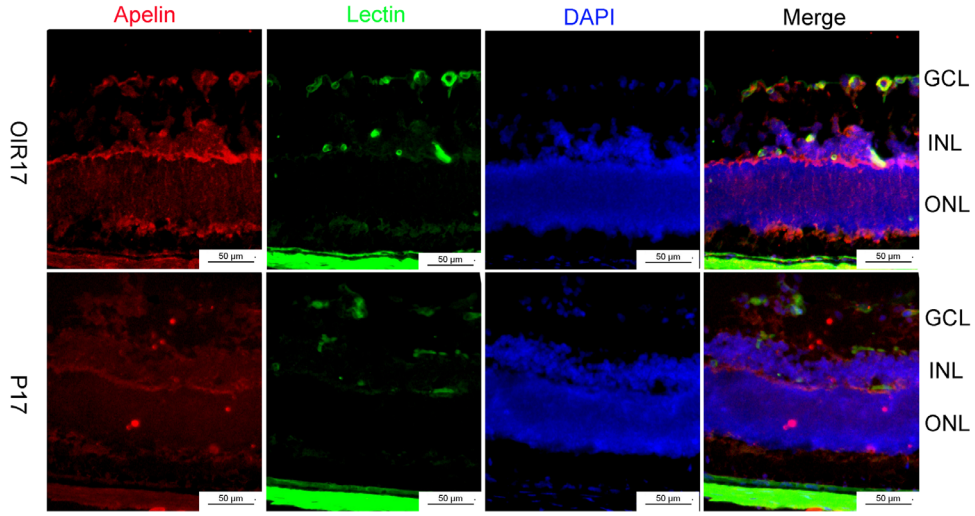

Figure 7. The expression of apelin in the normal mice and the OIR mice, both at P17. The expression of apelin was positive at P17 in the OIR model, where a visible strong red staining is distributed in the ganglion cell layer, inner nuclear layer, and the vessel wall. *GCL*, ganglion cell layer; *INL*, inner nuclear layer; *ONL*, outer nuclear layer; Scale bar = 100 μm.

in the OIR mice treated with F13A compared with the untreated OIR mice. Together, these findings suggest that the apelin/APJ system is a prerequisite in pathological retinal angiogenesis.

Angiogenesis is a multistep process, involving several interrelated reactions such as endothelial cell migration, proliferation, and capillary tube formation.[17] Apelin and APJ are known to be expressed in endothelium and smooth muscle cells; apelin is especially highly expressed in tip cells.[17] Similarly, apelin stimulated HUVEC and RF/6A cell migration, proliferation, and Matrigel tube formation.[21,22] These results suggested that apelin plays a key role in endothelial cells and vascularization. Interestingly, apelin mRNA is localized in tip cells: an endothelial subpopulation that forms cell protrusions and directs the polarized extension of the vascular network.[17] Meanwhile, these tip cells appear to respond to guidance cues conferring positional information,[23] which use dynamic filopodia to sense guidance cues in their surroundings to migrate.[24] Presently, VEGF-A is known as an important component for tip cell migration and proliferation, which depends on the gradient and concentration of VEGF-A.[25] Cox et al. proved that apelin peptide (10 ng/mL) was approximately equivalent to VEGF (50 ng/mL) in stimulation of angiogenic growth.[26] These data showed that apelin/APJ signaling plays a prerequisite role in regulating retinal vascularization.

In our study, we found that intraperitoneal injection of exogenous apelin promoted the superficial retinal vascular development for postnatal mice. Compared with PBS injection (control), the apelin-treated group had a larger retinal vessel area and a higher number of tip cells that were also

Investigative Ophthalmology & Visual Science

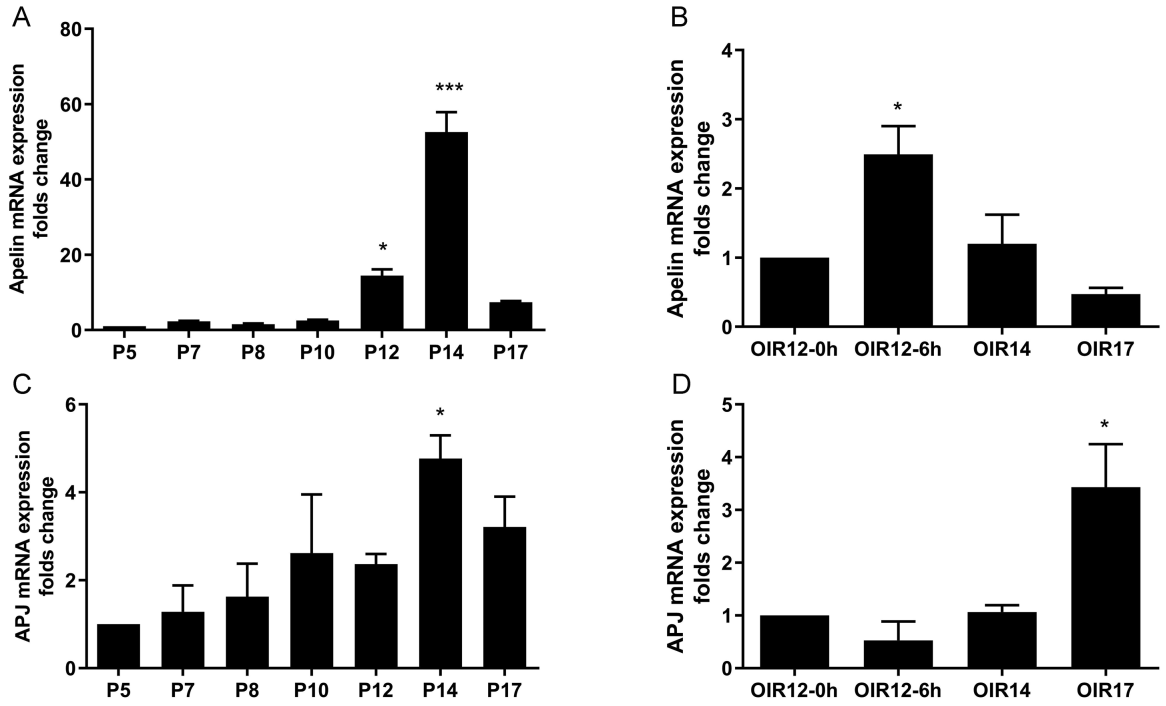

Figure 8. The qRT-PCR analysis of mRNA expression levels. The mRNA expression of apelin (**A, B**) and APJ (**C, D**) in mouse retina at normoxia conditions and in OIR mice was determined (*$P < 0.05$, ***$P < 0.001$).

longer in length. These findings were associated with the properties of apelin as an angiogenic factor, which stimulated endothelial mitogen, as well as enhanced proliferation, migration, and tube formation.[27] However, after the superficial vessels of the retina were formed, apelin had no effect on the mature vessels. Indeed, once at P10, there was no difference in the vessel area and vessel density between the apelin-treated and PBS-treated group. Nevertheless, apelin still stimulated the tip cell growth of deep retina vessels. Similar results have been reported by Kasai's study, in which the superficial retinal vascularization in apelin-KO mice was reduced at P5 and P7, whereas the vascularization of the deep retinal layer was reduced at P15, although it was completely restored at P84.[19] Moreover, previous study has shown that there was no apelin/APJ expression in mature blood vessels on the retina but that it was highly expressed in abnormal neovascularization.[17] Kasai et al. have proven that apelin also restricts pericyte recruitment, establishing a new connection between endothelial cell proliferation signaling and a trigger of mural cell recruitment.[5] This suggested that inhibition of the apelin/APJ system should block the development of abnormal blood vessels in the retina without impacting the growth of normal ones, which is different from anti-VEGF as it would impact the normal vessels as well. Ishimaru et al. also reported that APJ inhibitors selectively prevent the process of pathological retinal angiogenesis. In this regard, we believe that an anti-apelin/APJ signaling therapy may be superior over an anti-VEGF one.

Retinal hypoxia after P12 leads to increased proliferation of endothelial cells and pathological angiogenesis in OIR mice.[12] Here, we showed the expression of apelin and APJ expression in OIR mice. Additionally, the PCR results revealed that the expression of apelin peaked first (6 h post-return to ambient conditions at P12) and was followed later by APJ (at P17) in OIR mice. This was partly consistent with a previous report from Kasai et al.,[12] who showed that during the hypoxic phase, mRNA expression of apelin significantly increased by 31.18 ± 2.39 times in OIR mice at P15 and that mRNA expression of APJ in retinas abruptly increased at P17.

The intricate mechanism by which the apelin/APJ system involves in pathological angiogenesis in ROP remains largely unknown. It has been reported that apelin/APJ activates p70S6 kinase signaling through ERK1/2 and PI3K of Akt.[28] Eyries et al.[20] reported that in embryonic mouse endothelial cells cultured in hypoxia, the phosphorylation activity of p70s6 kinase to its mTOR was increased. Additionally, mTOR expression was increased as well. As such, by using siRNA to interfere with the apelin or APJ expression, the extent of p70s6 kinase phosphorylation and mTOR expression were significantly reduced, indicating that apelin combined with its receptor APJ can activate the p70s6 kinase.[20] Furthermore, mTOR knockdown, rapamycin, or Akt inhibition specifically and significantly inhibited the proliferation of endothelial cells under hypoxia.[29] Based on these findings, we also studied the expression of mTOR and its phosphorylated form in the OIR mice model. The results showed that the presence of p-mTOR increased under hypoxia. On top, the APJ antagonist F13A inhibited the ratio of p-mTOR: mTOR, indicating that mTOR was activated by apelin.

In summary, our data indicate that apelin promoted the physical vessel development in the retina, while having no effect on the mature vessels. It is an early promoter of neovascularization during the pathogenesis of OIR, which might offer a new perspective in strategies in the early prevention and treatment of ROP.

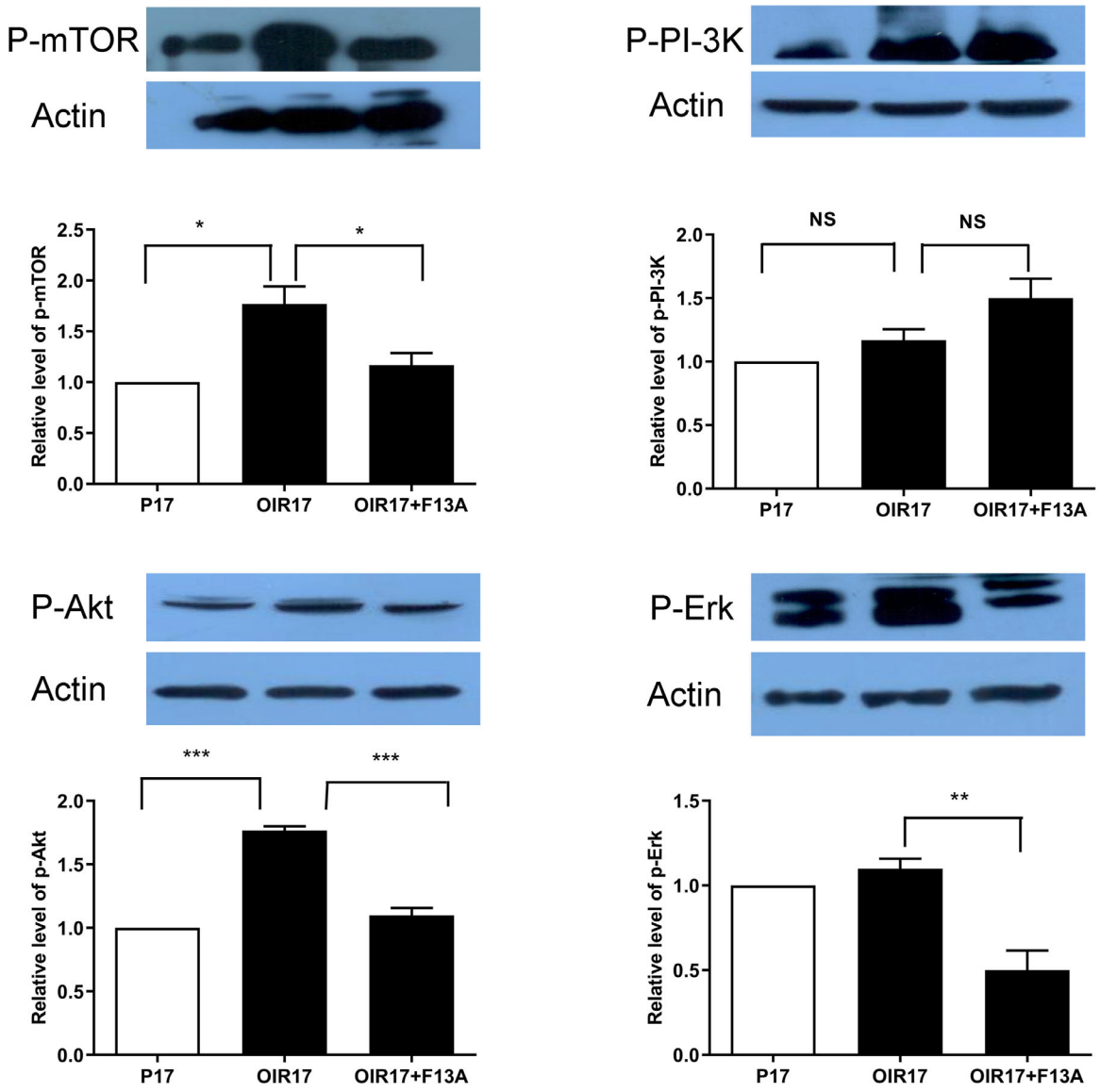

Figure 9. Western blot analysis. The protein expression of p-mTOR, p-Akt, and p-Erk were up-regulated in OIR mice and decreased after injection with the F13A antagonist (*$P < 0.05$, **$P < 0.01$, ***$P < 0.001$).

Acknowledgments

Supported by Beijing Municipal Science & Technology Commission (No. Z171100001017229) and Beijing Hospitals Authority Youth (No. QML20190303).

Disclosure: **J. Feng,** None; **L. Chen,** None; **Y. Jiang,** None; **Y. Tao,** None

References

1. Leske DA, Wu J, Mookadam M, et al. The relationship of retinal VEGF and retinal IGF-1 mRNA with neovascularization in an acidosis-induced model of retinopathy of prematurity. *Current Eye Research*. 2006;31:163–169.
2. Sato T, Kusaka S, Shimojo H, Fujikado T. Simultaneous analyses of vitreous levels of 27 cytokines in eyes with retinopathy of prematurity. *Ophthalmology*. 2009;116:2165–2169.
3. Mintz-Hittner HA, Kuffel RR, Jr. Intravitreal injection of bevacizumab (avastin) for treatment of stage 3 retinopathy of prematurity in zone I or posterior zone II. *Retina*. 2008;28:831–838.
4. Feng J, Qian J, Jiang Y, et al. Efficacy of primary intravitreal ranibizumab for retinopathy of prematurity in China. *Ophthalmology*. 2017;124:408–409.
5. Kasai A, Ishimaru Y, Higashino K, et al. Inhibition of apelin expression switches endothelial cells from proliferative to mature state in pathological retinal angiogenesis. *Angiogenesis*. 2013;16:723–734.
6. Hu J, Blair MP, Shapiro MJ, Lichtenstein SJ, Galasso JM, Kapur R. Reactivation of retinopathy of prematurity after bevacizumab injection. *Arch Ophthalmol*. 2012;130:1000–1006.
7. Wang H. Anti-VEGF therapy in the management of retinopathy of prematurity: what we learn from representative animal models of oxygen-induced retinopathy. *Eye Brain*. 2016;8:81–90.

8. Li Y, Bai YJ, Jiang YR, et al. Apelin-13 Is an Early Promoter of Cytoskeleton and Tight Junction in Diabetic Macular Edema via PI-3K/Akt and MAPK/Erk Signaling Pathways. *Biomed Res Int*. 2018;2018:3242574.
9. McKenzie JA, Fruttiger M, Abraham S, et al. Apelin is required for non-neovascular remodeling in the retina. *Am J Pathol*. 2012;180:399–409.
10. Feng J, Zhou Y, Zhang X, Jiang Y. Vascular endothelial growth factor and apelin in plasma of patients with retinopathy of prematurity. *Acta Ophthalmol*. 2017;95:e514–e515.
11. Zhang Y, Jiang YR, Lu Q, Yin H, Tao Y. Apelin in epiretinal fibrovascular membranes of patients with retinopathy of prematurity and the changes after intravitreal bevacizumab. *Retina*. 2013;33:613–620.
12. Kasai A, Ishimaru Y, Kinjo T, et al. Apelin is a crucial factor for hypoxia-induced retinal angiogenesis. *Arterioscler Thromb Vasc Biol*. 2010;30:2182–2187.
13. Kalin RE, Kretz MP, Meyer AM, Kispert A, Heppner FL, Brandli AW. Paracrine and autocrine mechanisms of apelin signaling govern embryonic and tumor angiogenesis. *Dev Biol*. 2007;305:599–614.
14. Smith LE, Wesolowski E, McLellan A, et al. Oxygen-induced retinopathy in the mouse. *Investigative Ophthalmology & Visual Science*. 1994;35:101–111.
15. Connor KM, Krah NM, Dennison RJ, et al. Quantification of oxygen-induced retinopathy in the mouse: a model of vessel loss, vessel regrowth and pathological angiogenesis. *Nat Protoc*. 2009;4:1565–1573.
16. Xu Z, Gong J, Maiti D, et al. MEF2C ablation in endothelial cells reduces retinal vessel loss and suppresses pathologic retinal neovascularization in oxygen-induced retinopathy. *Am J Pathol*. 2012;180:2548–2560.
17. Saint-Geniez M, Masri B, Malecaze F, Knibiehler B, Audigier Y. Expression of the murine msr/apj receptor and its ligand apelin is upregulated during formation of the retinal vessels. *Mech Dev*. 2002;110:183–186.
18. Stahl A, Connor KM, Sapieha P, et al. The mouse retina as an angiogenesis model. *Invest Ophthalmol Vis Sci*. 2010;51:2813–2826.
19. Kasai A, Shintani N, Kato H, et al. Retardation of retinal vascular development in apelin-deficient mice. *Arterioscler Thromb Vasc Biol*. 2008;28:1717–1722.
20. Eyries M, Siegfried G, Ciumas M, et al. Hypoxia-induced apelin expression regulates endothelial cell proliferation and regenerative angiogenesis. *Circ Res*. 2008;103:432–440.
21. Kasai A, Shintani N, Oda M, et al. Apelin is a novel angiogenic factor in retinal endothelial cells. *Biochem Biophys Res Comm*. 2004;325:395–400.
22. Kunduzova O, Alet N, Delesque-Touchard N, et al. Apelin/APJ signaling system: a potential link between adipose tissue and endothelial angiogenic processes. *FASEB J*. 2008;22:4146–4153.
23. Samakovlis C, Hacohen N, Manning G, Sutherland DC, Guillemin K, Krasnow MA. Development of the Drosophila tracheal system occurs by a series of morphologically distinct but genetically coupled branching events. *Development*. 1996;122:1395–1407.
24. Ribeiro C, Ebner A, Affolter M. In vivo imaging reveals different cellular functions for FGF and Dpp signaling in tracheal branching morphogenesis. *Dev Cell*. 2002;2:677–683.
25. Gerhardt H, Golding M, Fruttiger M, et al. VEGF guides angiogenic sprouting utilizing endothelial tip cell filopodia. *J Cell Biol*. 2003;161:1163–1177.
26. Cox CM, D'Agostino SL, Miller MK, Heimark RL, Krieg PA. Apelin, the ligand for the endothelial G-protein-coupled receptor, APJ, is a potent angiogenic factor required for normal vascular development of the frog embryo. *Dev Biol*. 2006;296:177–189.
27. Kasai A, Shintani N, Oda M, et al. Apelin is a novel angiogenic factor in retinal endothelial cells. *Biochem Biophys Res Commun*. 2004;325:395–400.
28. Masri B, Morin N, Cornu M, Knibiehler B, Audigier Y. Apelin (65-77) activates p70 S6 kinase and is mitogenic for umbilical endothelial cells. *FASEB J*. 2004;18:1909–1911.
29. Li W, Petrimpol M, Molle KD, Hall MN, Battegay EJ, Humar R. Hypoxia-induced endothelial proliferation requires both mTORC1 and mTORC2. *Circ Res*. 2007;100:79–87.